

A fast and simple method of spectral enhancement

Muhammad Sajid¹ and Deva Ghosh¹

ABSTRACT

The ability to resolve seismic thin beds is a function of the bed thickness and the frequency content of the seismic data. To achieve high resolution, the seismic data must have broad frequency bandwidth. We developed an algorithm that improved the bandwidth of the seismic data without greatly boosting high-frequency noise. The algorithm employed a set of three cascaded difference operators to boost high frequencies and combined with a simple smoothing operator to boost low frequencies. The output of these operators was balanced and added to the original signal to produce whitened data. The four convolutional operators were quite short, so the algorithm was highly efficient. Synthetic and real data examples demonstrated the effectiveness of this algorithm. Comparison with a conventional whitening algorithm showed the algorithm to be competitive.

INTRODUCTION

Many petroleum reservoirs are at or below the limit of seismic resolution, making it difficult to determine their thickness. To better resolve these reservoirs, it is necessary to make full use of the available signal bandwidth, as greater bandwidth implies a shorter signal and higher resolution. To this end, several methods have been developed to enhance the bandwidth, such as spectral whitening, spectral bluing, and inverse Q-filtering (Hargreaves and Calvert, 1991; Fraser and Neep, 2004; Kazemeini et al., 2008; Yilmaz, 2008, pp. 231–233). These methods work well, but they require specific parameterization, and in some cases they are computationally expensive.

We develop an algorithm based on a set of cascaded dipole filters (Claerbout [2004], pp. 9–10), which we call *differential resolution* (DR), to improve seismic resolution through spectral whitening. The algorithm requires no parameterization and is much faster than

competing algorithms for spectral whitening. Tests on synthetic and real seismic data demonstrate its efficiency and effectiveness. It is well-suited for application in tools for interpretive data processing, in which computational speed and simplicity of implementation are paramount.

METHOD

The DR algorithm adds the original seismic trace to a smoothed version of the trace, and also adds the second-, fourth-, and sixth-order differentiated versions of the trace. For efficiency, we accomplish differentiation with difference operators. Each order of difference has a higher-dominant frequency. Adding the smoothed trace boosts low frequencies, and adding the three difference traces boosts high frequencies. The net effect is to enhance the entire bandwidth of the data.

Each difference introduces a -90° phase shift. Thus, the fourth-order difference trace has normal polarity but the second- and sixth-order difference traces have reverse polarity and so are multiplied by -1 in the addition. The amplitude of each difference trace is normalized with respect to its median value of the absolute value of amplitudes:

$$Y = \frac{X}{|\tilde{X}|}, \quad (1)$$

where X is the input seismic trace, $|\tilde{X}|$ is the median of the absolute value of X , and Y is the normalized seismic trace.

The normalized traces are added together to produce a whitened trace that itself is normalized:

$$r = Y + Y_s - Y^{II} + Y^{IV} - Y^{VI}, \quad (2)$$

where Y^j is the normalized j th-order differential of Y , Y_s is the smooth version of Y , and r is the nonnormalized DR:

$$R = \frac{r}{|r|}, \quad (3)$$

Manuscript received by the Editor 9 May 2013; revised manuscript received 24 November 2013; published online 28 March 2014.

¹Universiti Teknologi PETRONAS, Geoscience and Petroleum Engineering Department, Tronoh, Malaysia. E-mail: geosajid@gmail.com; drdeva@petronas.com.my.

© 2014 Society of Exploration Geophysicists. All rights reserved.

where $\tilde{|r|}$ is the median of the absolute value of r and R is the normalized DR.

The smoothed version of the trace is obtained by 10 passes of the three point smoother with weights [1 2 1]. The algorithm works trace by trace.

An ideal differentiator boosts high frequencies linearly relative to low frequencies and has the amplitude spectrum $D(f)$ given by

$$D(f) = |2\pi f|, \tag{4}$$

where $D(f)$ is the amplitude spectrum derivative and f is the frequency.

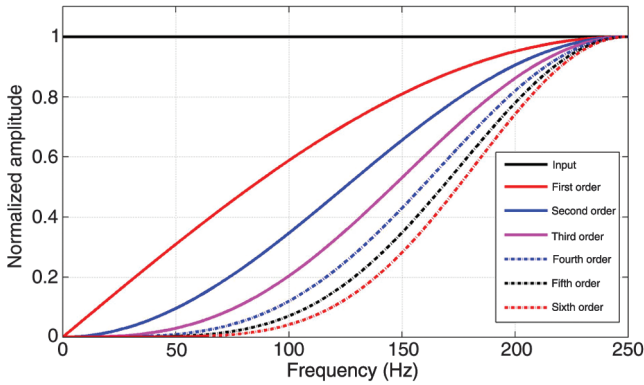


Figure 1. Amplitude spectrum of the input spike and its first- to sixth-order differential output shows nonlinear behavior of the differentials.

Figure 1 shows the amplitude spectrum of the input spike by the black constant line and its first- through sixth-order differential operators. These amplitude spectrums are normalized to one for comparison. The input spike contains all the frequencies (i.e., zero to Nyquist frequency), whereas these operators have nonlinear behavior which suppresses the low frequencies and this suppression increases with the order of differential. The rate of high-frequency boost is also nonlinear and decreases with the order of the difference. This effect can be observed by comparing the distance between the two consecutive amplitude-spectrum curves. This property of the difference operator minimizes the high-frequency noise boost effect of the derivative.

The first-order derivative of the signal y with respect to time t , for constant sample interval Δt , is approximated by the forward difference,

$$y'_j \cong \frac{y_{j+1} - y_j}{\Delta t} (j \in R(1 \geq j \geq n - 1)). \tag{5}$$

The second-order derivative is approximated by applying two successive difference operations on the signal $y(t)$, one a forward difference and the other a backward difference such that combined they introduce no time shift. The same strategy is followed for higher-order derivatives. Figure 2a shows the normalized input trace, second-, fourth-, and sixth-differential output in blue, green, magenta, and black color, respectively and Figure 2c shows their respective amplitude spectra. Each difference operation shifts the dominant frequency toward higher frequencies.

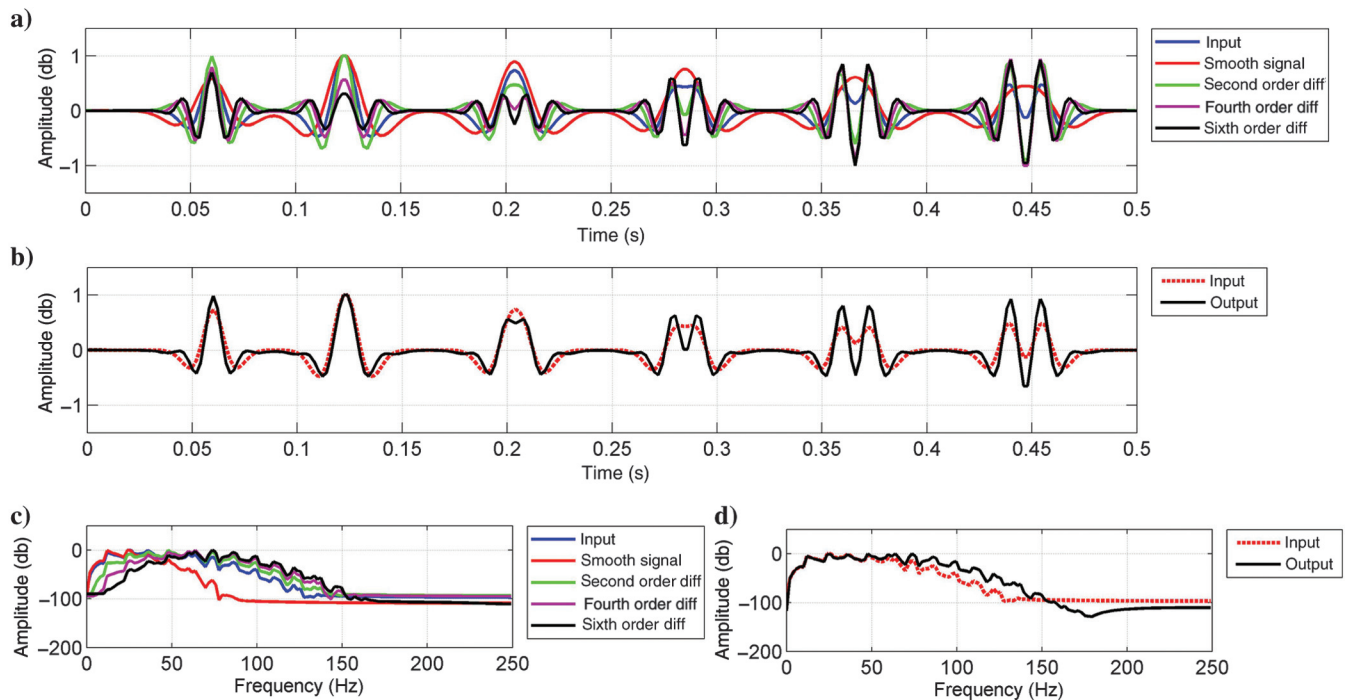


Figure 2. (a) Input variables of DR algorithm showing the input thin-bed model, its smoothed version, and the output of the second-, fourth-, and sixth-order difference operators, (b) DR resolves the events below the original tuning thickness, (c) the amplitude spectrum of DR components, and (d) comparison of original spectrum with whitened spectrum showing that low frequencies are preserved and high frequencies are enhanced.

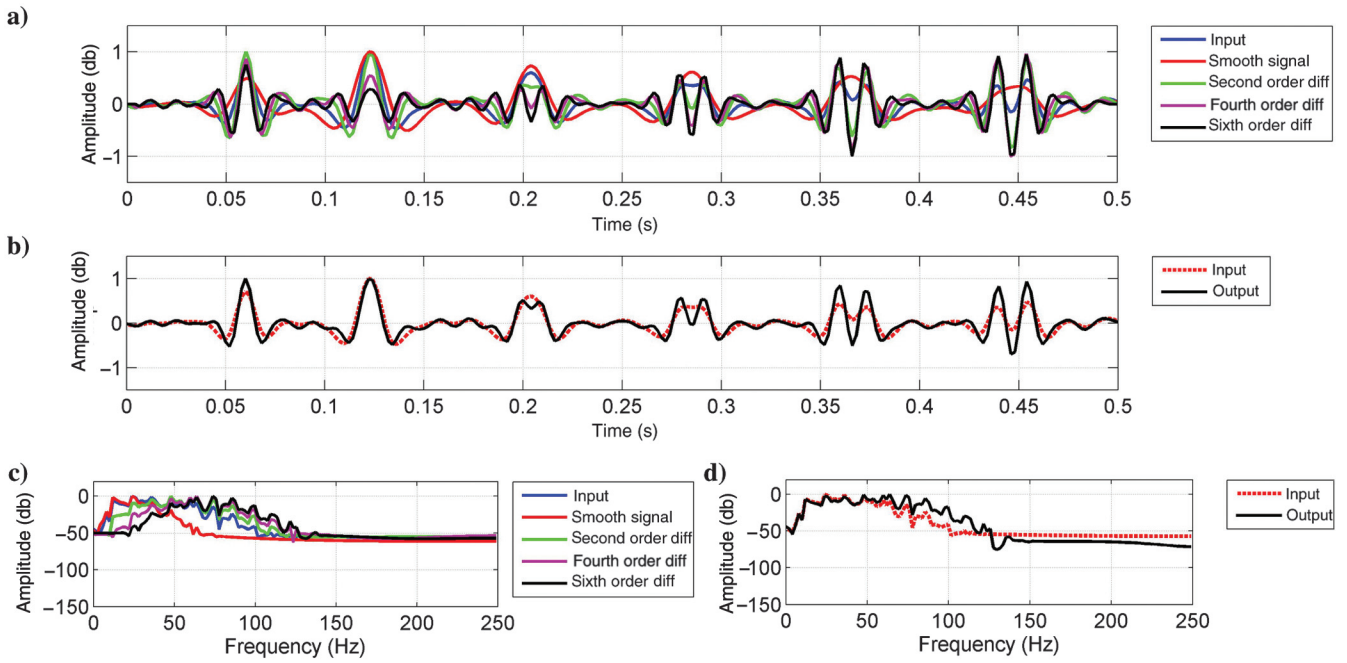


Figure 3. (a) Input variable of the DR algorithm for thin-bed model with band limited noise (S/N = 4), (b) comparison of DR with original input shows the improved waveform hidden information, (c) the amplitude spectrum of each DR component, and (d) comparison of amplitude spectrum shows that the low frequency is preserved, whereas the high frequency is broadened.

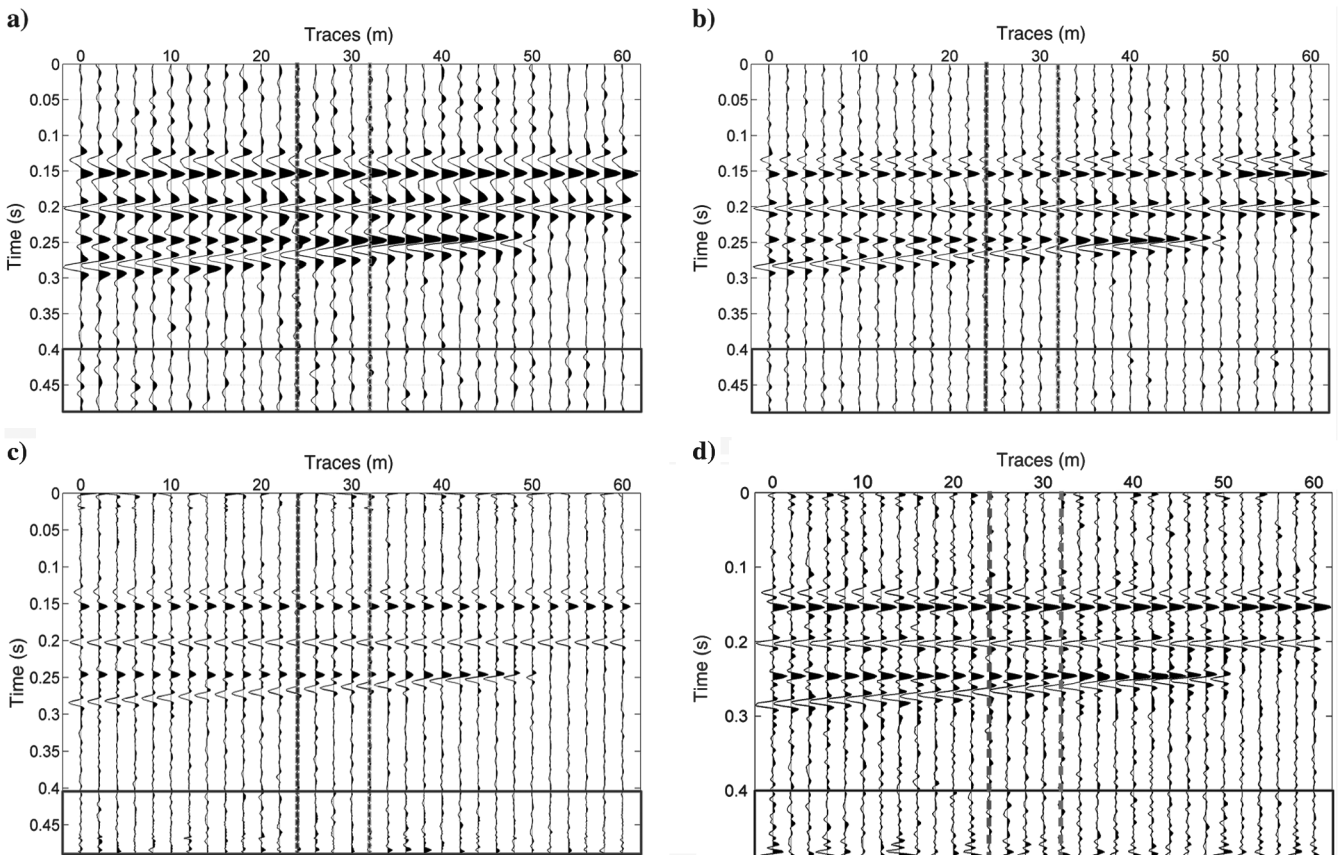


Figure 4. (a) Synthetic seismic wedge model with the trace interval of 2 m and S/N of 3, (b) events started to merge at trace number 24 are still separable till trace 32 (i.e., 8-m increase in resolution), (c) shows Gabor deconvolution output, DR algorithm resolution is comparable with Gabor deconvolution but in less time, and (d) spectral whitening algorithm output, DR algorithm resolution is comparable with spectral whitening with comparatively less boost in noise.

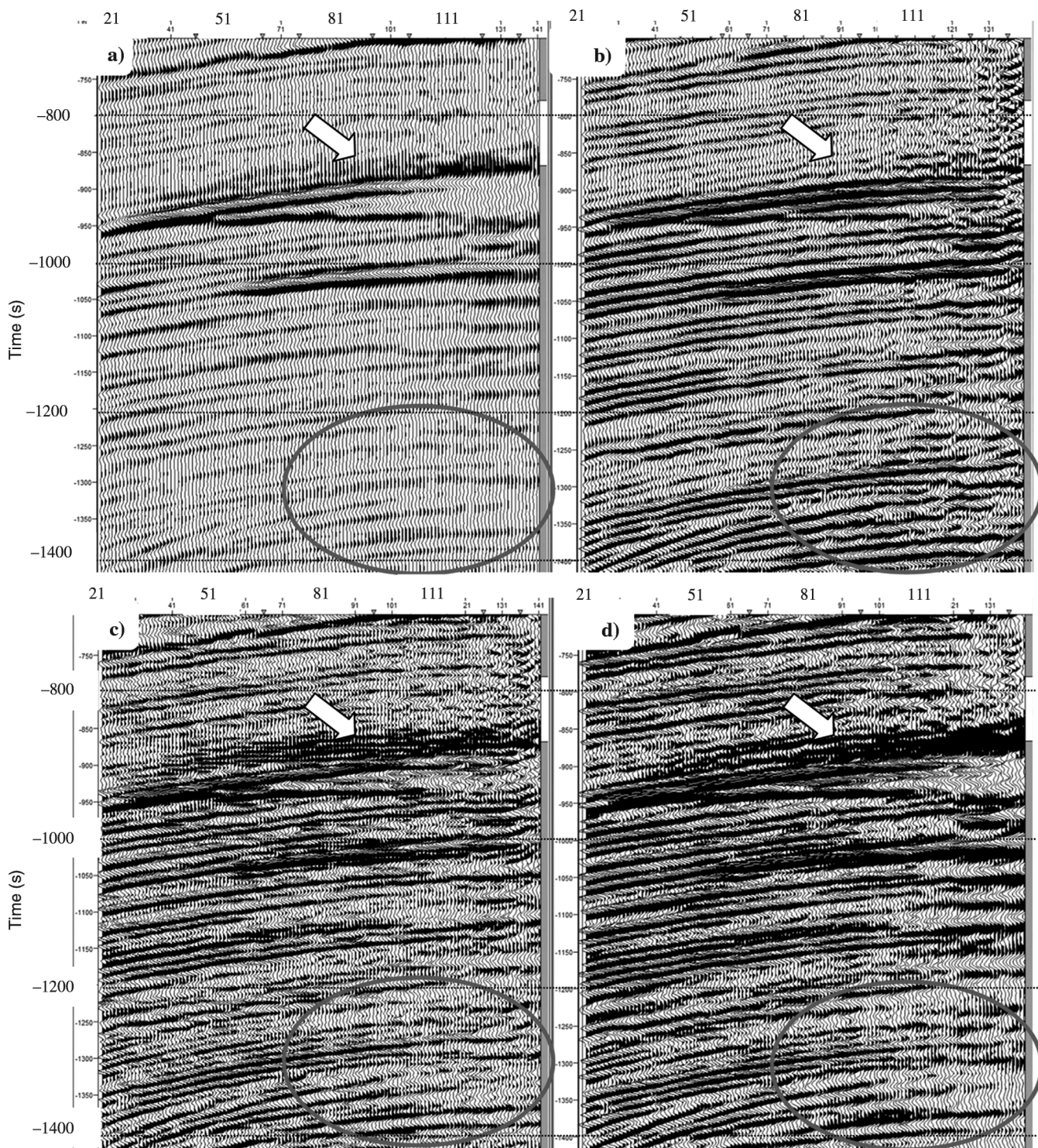


Figure 5. (a) Real seismic section from Malay basin, containing hidden and thin-bed features, (b) after the application of DR algorithm, resolution of the seismic is greatly improved and hidden features are recovered, (c) real seismic after the application of Gabor-deconvolution shows nonrealistic features shown by the arrow sign, and (d) spectral whitening algorithm output unable to resolve the thin-bed and hidden features shown by arrow sign and red oval.

RESULTS

Application of DR on a synthetic trace

Figure 2 illustrates the application of the algorithm to a synthetic trace that comprises a set of six thin-bed models for the following conditions:

- 1) Single event wavelet ($f_{\text{dom}} = 35$ Hz and tuning thickness = 12 ms).
- 2) Two events are in between zero and flat spot thickness (three samples or 6 ms thickness).
- 3) Two events are below flat spot thickness (four samples or 8 ms thickness).
- 4) Flat spot thickness (five samples or 10 ms thickness) (Ricker's [1953] criterion).
- 5) Tuning thickness (six samples or 12 ms thickness) (Rayleigh's criterion) (Kallweit and Wood, 1982).
- 6) Greater than tuning thickness (seven samples or 14 ms thickness).

Figure 2a shows the input variables of the DR algorithm, whereas Figure 2b shows the comparison of original input with DR algorithm output, demonstrating a considerable increase in the event resolution at and below the tuning thickness. Figure 2c shows the comparison between the amplitude spectrum of the input variables of the DR algorithm, whereas Figure 2d shows the comparison of the amplitude spectrum of the thin-bed model before and after the application of the proposed algorithm. Similarly, Figure 3 shows the application of the DR algorithm on thin-bed model with normally distributed band limited noise with a signal-to-noise ratio (S/N) of 4.

The DR algorithm does not add frequencies but instead boosts existing frequencies to broaden the amplitude spectrum and reveal hidden features. Amplitude spectrum is broadened by the addition of higher-order derivatives of signal and through the preservation of low frequencies by addition of the original and its low-frequency (i.e., smooth version) output.

Application of the DR on the 2D synthetic wedge model

The 2D synthetic model is created from the geological model of the stratigraphic layer of the known thickness and elastic properties. In the synthetic seismic shown in Figure 4a, trace interval is 2 m, sample rate is 2 ms, the wedge layer velocity is 2700 m/s, and

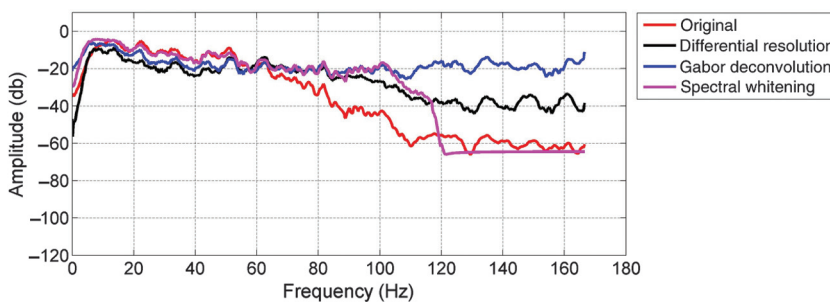


Figure 6. The comparison of the amplitude spectrum of DR algorithm output with the amplitude spectrum of original seismic, Gabor deconvolution algorithm output and spectral whitening algorithm.

Ricker wavelet with the predominant frequency of 35 Hz (tuning thickness $b_{\text{time}} = 12$ ms or $b_{\text{space}} = 2700$ m/s \times (0.012/2) s, $b_{\text{space}} = 16.2$ m) is used. Figure 4b shows the synthetic seismic after the application of the DR algorithm. Lines are drawn for comparison purposes. The horizontal interface of the two layers is better to resolve after the application of the DR algorithm. In wedge model, where the interfaces start merging at the trace number 24 are still separable till trace number 32 after the application of DR algorithm, which shows 8-m increase in resolution (i.e., 50% decrease in resolution limit) without greater boost in seismic noise. Similarly Figure 4c and 4d shows the 2D synthetic seismic section after the application of Gabor deconvolution and spectral whitening algorithm. This analysis shows that the resolution achieved through DR is comparable to Gabor deconvolution but takes comparatively less time, whereas in comparison with spectral whitening algorithm, DR algorithm handles the noise boost more effectively.

Application of DR algorithm on a real seismic event

Figure 5 shows the application of the DR algorithm on real seismic from the Malay Basin, which images carbonates, and compares this with Gabor deconvolution and spectral whitening. Gabor deconvolution is equivalent to Wiener filtering with a nonstationary wavelet that compensates for Q (Perz et al., 2005; Margrave et al., 2011). The spectral whitening is accomplished through a standard commercial algorithm, and has corner frequencies of 1, 5, 90, and 120 Hz (Yilmaz [2008], p. 231–233). DR considerably increases the resolution of the thin-bed sand and reveals hidden features, as marked by an arrow. Spectral whitening broadens the amplitude spectrum to fit the desired bandwidth, which typically enhances high-frequency noise. The DR algorithm is less susceptible to this problem as its operators flatten out at high frequencies. The DR algorithm is simple and fast. Figure 6 shows the comparison of their amplitude spectrum. DR algorithm effectively preserves the low frequencies of the seismic through its original and smooth version of the input signal, whereas the frequency spectrum is broadened without the influence of user defined boundaries.

CONCLUSION

The vertical resolution of seismic data is a function of its frequency content. When seismic reflections interfere with each other in a thin bed, they become difficult to resolve, and below the tuning thickness of the seismic wavelet they become inseparable. The DR algorithm helps to resolve thin beds by expanding the bandwidth of the seismic data. The amplitude spectra of the seismic data after DR algorithm follow the trend and behavior as the input seismic data, but with the high frequencies boosted. The algorithm is fast and requires no user-defined parameters. Tests on the 1D synthetic thin-bed model, 2D synthetic-wedge model, and on 3D seismic volume with different characters demonstrate its efficiency and effectiveness to improve seismic resolution in general applications.

ACKNOWLEDGMENTS

We thank Universiti Teknologi PETRONAS (UTP) for providing the resources for research and PETRONAS for support and permission to show seismic data of Malay Basin. M. Sajid thanks University Commission on Science and Technology for Sustainable Development in South (www.ciit.net.pk) for providing the opportunity to carry out research at UTP. We also thank professor Haver from the University of Maryland, Arthur E. Barnes, and M. Brewer from PETRONAS for valuable discussion and suggestions. We use the Consortium for Research in Elastic Wave Exploration Seismology free software package and Kingdom from Seismic Micro-Technology for Gabor deconvolution and spectral whitening, respectively, in our comparison of algorithms.

REFERENCES

- Claerbout, J. F., 2004, *Earth soundings analysis: Processing versus inversion*: Blackwell Scientific Publications, 9–10.
- Fraser, G. B., and J. Neep, 2004, Increasing seismic resolution using spectral blueing and colored inversion: Cannonball field, Trinidad: 74th Annual International Meeting, SEG, Expanded Abstracts, 1794–1797.
- Hargreaves, N., and A. Calvert, 1991, Inverse Q filtering by Fourier transform: *Geophysics*, **56**, 519–527, doi: [10.1190/1.1443067](https://doi.org/10.1190/1.1443067).
- Kallweit, R. S., and L. C. Wood, 1982, The limits of resolution of zero-phase wavelets: *Geophysics*, **47**, 1035–1046, doi: [10.1190/1.1441367](https://doi.org/10.1190/1.1441367).
- Kazemeini, S. H., S. Fomel, and C. Juhlin, 2008, Prestack spectral blueing: A tool for increasing seismic resolution: 78th Annual International Meeting, SEG, Expanded Abstracts, 854–858.
- Margrave, G., M. Lamoureux, and D. Henley, 2011, Gabor deconvolution: Estimating reflectivity by nonstationary deconvolution of seismic data: *Geophysics*, **76**, no. 3, W15–W30, doi: [10.1190/1.3560167](https://doi.org/10.1190/1.3560167).
- Perz, M., L. Mewhort, G. Margrave, and L. Ross, 2005, Gabor deconvolution: Real and synthetic data experiences: 75th Annual International Meeting, SEG, Expanded Abstracts, 494–497.
- Ricker, N., 1953, Wavelet contraction, wavelet expansion, and the control of seismic resolution: *Geophysics*, **18**, 769–792, doi: [10.1190/1.1437927](https://doi.org/10.1190/1.1437927).
- Yilmaz, O., 2008, *Seismic data analysis*: SEG, vol. 1, 231–233.